SQU Journal for Science, 2017, 22(1), 16-28 DOI: http://dx.doi.org/10.24200/squjs.vol22iss1pp16-28

Study on the Reactivity of Amino Acid Chemosensor, NPFNP, with Ethanol: Structural Elucidation through Single Crystal XRD and DFT Calculations

Beena Varghese, Saleh N. Al-Busafi*, Fakhr Eldin O. Suliman* and Salma Al-Kindy

*Department of Chemistry, College of Science, Sultan Qaboos University, P.O. Box 36, PC 123, Al-Khoud, Muscat, Sultanate of Oman. *Email:Saleh1@squ.edu.om; fsuliman@squ.edu.om.*

ABSTRACT: A novel ethoxy derivative of an amino acid chemosensor, 3-naphthyl-1-phenyl-5-(2′-fluoro-5′-nitrophenyl)-2-pyrazoline (NPFNP), has been synthesized and characterized by different spectroscopic methods. A single crystal of the ethoxy derivative, 3-naphthyl-1-phenyl-5-(2′-ethoxy-5′-nitrophenyl)-2-pyrazoline NPENP, has been obtained and characterized. The structure holds interest as it carries biologically active pyrazoline as a central ring attaching to electron donating and withdrawing substituents. The major motivation for this work was to gain detailed insight into the structural parameters of this compound for investigating the influence of crystal packing and geometrical dimensions on optical properties. Time-dependent DFT calculations have been employed for comparing the XRD data with theoretical parameters. The results show that the DFT method at B3LYP/6-31G level can well reproduce the structure of the title compound.

Keywords: Pyrazoline; UV absorption; Crystal structure; Chemosensor; TD-DFT.

دراسة تفاعل كاشف الأحماض الأمينيه (NPFNP) مع الإيثانول: كشف التركيب الجزيئي عن طريق استخدام الأشعة السينية (XRD) للبلورات وقياسات الكثافة الإلكترونيه (DFT)

بينا فيرجاس، صالح البوصافي، فخر الدين سليمان وسلمى الكندي

الملخص: لقد تم تحضير ومعرفة التركيب الجزيئي لمشتقة الإثوكسي (NPENP) لكاشف الأحماض الأمينيه (NPFNP) باستخدام أجهزة السبكتروسكوبي المختلفه. وأيضا، تم تحضير بلورة نقيه لمشتقة الإثوكسي ومن خلال استخدام الأشعه السينيه تم الكشف، ولأول مرة، عن التركيب الثلاثي الأبعاد لكاشف الأحماض الأمينيه (NPFNP). إن أهمية هذا العمل تنبع من محاولة تتبع العلاقة بين التركيب الثلاثي الأبعاد لبلورات الكاشف من جهة و خصائصه الضوئية من جهة أخرى. لقد تم استخدام العمليات الحسابيه المتعلقه بنظرية الكثافة الإلكترونية لمقارنة القراءات الناتجة عن استخدام الأشعة السينيه مع القراءات النظرية. نتائج المقارنة تشير الى امكانية الإعتماد إلى الحسابات النظرية لمعرفة الركيب الثلاثي الأبعاد للكاشف.

الكلمات مفتاحية: بيرازولين، امتصاص فوق البنفسجي، تركيب بلوري، كاشف كيميائي، ت د- د ف ت.

1. Introduction

The rising prevalence of heterocyclic compounds in bio-analytical chemistry has attracted the increasing attention of researchers to pyrazoline derivatives. Easily tunable properties suit these electron rich nitrogen heterocycles to be used extensively as useful synthons in organic synthesis [1-2] as well as for medicinal applications [3-4]. These significant key motifs in heterocyclic chemistry are known not only from their pharmaceutical applications but also as materials showing excellent optical properties. Moreover, the synthesis of fluorophores with desirable properties based on a pyrazoline skeleton is of considerable interest in fluorescent materials research [5-8]. A lot of work has been focused on the synthesis, crystal structure, optical properties and quantum chemical calculations of novel pyrazoline derivatives [9-12].

The hydroxyl group is a functional element of many drugs and naturally occurring compounds; however, its detection is still a challenging analytical subject [13]. To date there have been relatively few compounds capable of tagging the hydroxyl groups directly. This inadequacy observed in the literature encouraged us to address this

issue. Very recently, 3-naphthyl-1-phenyl-5-(5′-fluoro-2′-nitrophenyl)-2-pyrazoline was synthesized and characterized by our group and this probe showed a good affinity towards amino acid groups [14]. As a continuation of the mentioned study, we inspected the preparation and usability of 3-naphthyl-1-phenyl-5-(2′-fluoro-5′-nitrophenyl)-2-pyrazoline NPFNP, a constitutional isomer of the reported probe in which the fluorine atom is situated at carbon-2′ and the nitro group at carbon-5′ (see Figure 1).

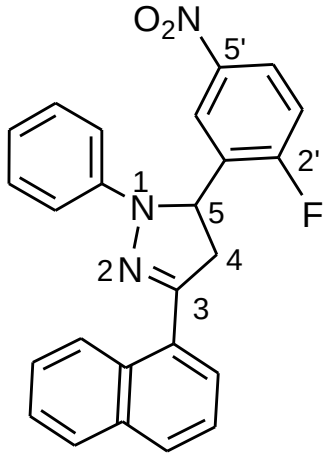

Figure 1. Structure of NPFNP.

In the present study we focus attention on the reactivity of NPFNP with a –OH group by reacting the probe with ethanol and aim to understand the structural details of the ethoxy product, 3-naphthyl-1-phenyl-5-(2′-ethoxy-5′-nitrophenyl)-2-pyrazoline NPENP in the solid state by means of X-ray crystallography (see Figure 2). Molecular geometries of NPENP in both ground and excited states have been calculated using the density functional theory, and the trend of calculated HOMO-LUMO gaps and geometrical parameters in excited state provides valuable information on the factors influencing the optical properties of NPENP.

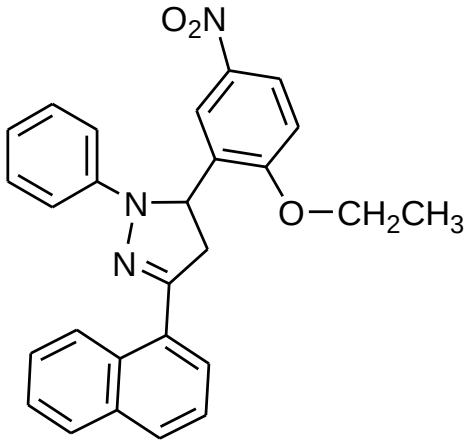

Figure 2. Structure of NPENP.

2. Experimental

All reagents and solvents used in this study were obtained from Sigma Aldrich Chemical Company and were used without further purification.

Melting point was determined using GallenKamp MPA350 melting point apparatus. The purity of the synthesised compounds was checked by TLC and analyses were carried out on 0.25 mm thick pre coated silica plates (Merck Fertigplatten Kieselgel $60F_{254}$). Column chromatography was performed using Merck silica gel 60 (40-63 µm). IR spectra were determined on a Cary 630 FTIR spectrometer (Agilent Technologies, USA). ^{1}HNMR and ^{13}CNMR spectra were recorded using a 400 MHz Bruker spectrometer (Bruker Corp., UK). Chemical shifts (δ_c) are quoted in parts per million (ppm) to the nearest 0.1 and 0.01 and are referenced to the solvent peak ($CDCl_3$). Mass spectra were obtained using a Quattro Ultima Pt tandem quadrupole mass spectrometer (Waters Corp. MA, USA). A Shimadzu

(model multispec-1501) UV-Vis spectrophotometer (Shimadzu, Japan) was used to collect absorption spectra. All measurements were done repeatedly, and reproducible results were obtained.

The single crystal suitable for X-ray measurements was obtained by recrystallization from hot ethanol. The selected golden yellow crystal (0.350 x 0.300 x 0.250 mm^3) of the compound was mounted on a Bruker AXS KAPPA APEX-II diffractometer at 293 (2) K with a graphite monochromatic Mo-K_α radiation (k = 0.71073 Å). The corrections for L_P factors and empirical absorption were applied to the data. The structures were solved by direct methods and refined by the full-matrix least-squares method F_{obs}^2 using the SHELXTL software package [15].

All non-H atoms were anisotropically refined. The anisotropic displacement factor exponent takes the form of $-2\pi^2 [h^2 a^{*2} U^{11} + ... + 2 h k a^* b^* U^{12}]$.

The hydrogen atom positions were fixed geometrically at calculated distances and allowed to ride on the parent C atoms. The final least-squares cycle gave R= 0.0975 and wR_2 = 0.254 for 3547 independent reflections [R (int) = 0.0896]. Atomic scattering factors and anomalous dispersion corrections were taken from International Table for X-ray crystallography [16].

The quantum chemical calculations were carried out with GAUSSIAN 09W programs and GaussView 05 was used for visualization of structures. DFT (Density Functional Theory) calculations were performed by using a combination of Becke's three parameter hybrid exchange potential [17] with the correlation functional of Lee *et al*. (B3LYP) [18]. The basis set used was 6-31G.

2.1 Synthesis of Compounds 3 and 5

2.1.1 Synthesis of (E)-3-(2′-fluoro-5′-nitrophenyl)-1-(naphthalene-5-yl)prop-2-en-1-one (3)

A mixture of 1-(naphthalene-4-yl)ethanone **1** (5.0 g, 29.4 mmol), 2-fluoro-5-nitro benzaldehyde **2** (5.0 g, 29.5 mmol) in 60 mL acetonitrile and aqueous potassium bicarbonate (5.2 g, 37.6 mmol) was refluxed for 2 hours. After stirring at room temperature for another 24 hours, the crude product was filtered and recrystallized from ethanol to give product **3** (3.6 g, 72.2 %) as an orange solid. Mp: 127-128 ^oC; IR (KBr): υ 3083, 1664, 1603, 1214, 857, 554 cm^{-1}; ^1H NMR (400 MHz, $CDCl_3$): δ (ppm) 7.64 (d, *J*= 8 Hz, 1H), 7.92 (d, *J*=16.8 Hz, 1H), 8.19 (dd, J_1=14.8 Hz, J_2=21.2 Hz); ^{13}CNMR (100.6 MHz, $CDCl_3$): δ (ppm) 129.05, 128.61, 126.59, 124.81. ESI-MS $[M + H]^+$ calculated for $C_{19}H_{12}FNO_3$: 322.3, found: 322.1.

2.1.2 Synthesis of 3-naphthyl-1-phenyl-5-(2′-ethoxy-5′-nitrophenyl)-2-pyrazoline (NPENP)

A solution of (*E*)-3-(2′-fluoro-5′-nitrophenyl)-1-naphthyl-prop-2-en-1-one **3** (2.5 g, 7.40 mmol) and phenyl hydrazine (1.2 g, 11.1 mmol) in ethanol (25 ml) was kept refluxing for 2 hours. After stirring at room temperature for another 24 hours, the crude product was filtered and re-crystallized from hot ethanol to give product **5** (2.5 g, 77.16%) as golden yellow crystals; Mp:184-185 ^oC; FTIR: υ 1025, 1254, 1325, 1496,1786 cm^{-1}; ^1H NMR (400 MHz, $CDCl_3$): δ (ppm) 1.49 (t, *J*=6.9, 3H), 3.20 (dd, *J*=7.0, 16.9 Hz, 1H), 4.05 (dd, *J*=12.4, 16.9 Hz,1H), 4.21 (q, *J*=7.0 Hz,2H), 5.52 (dd, *J*=7.0, 12.4 Hz,1H), 7.47-9.54 (m, Aromatic hydrogens); ^{13}C NMR (100.6 MHz, $CDCl_3$): δ (ppm) 15.1, 42.1, 58.0, 65.3, 113.7, 120.0-148.4, 161.0. ESI-MS [M+H calculated for $C_{27}H_{23}N_3O_3$: 438.48, found: 438.2.

3. Results and Discussion

3.1 Synthesis and ^1H NMR characterization of NPENP

The synthesis of NPENP commenced from an aldol reaction between 1-acetylnaphthalene **1** and 2′-fluoro-5′-nitro benzaldehyde **2** in acetonitrile using sodium carbonate as a base to give α,β-unsaturated ketone **3** in 72 % yield. A cyclization reaction of compound **3** with phenylhydrazine in refluxing ethanol led to the formation of the pyrazoline derivative **4** which reacted *in situ* with ethanol to yield its ethoxy derivative **5** (Scheme 1). The synthetic route adopted was straightforward, and NPENP was obtained by following aromatic nucleophilic substitution, in which a NO_2 group stabilises the anion intermediate through resonance, and the fluorine atom *para* to -NO_2 can be easily replaced by the –OH group of the ethanol to yield the desired ethoxy derivative.

The ^1H NMR spectrum of the eight aliphatic hydrogens in NPENP displayed in Figure 3 exhibits three equally intense doublet of doublets, each accounting for one hydrogen atom on the pyrazoline ring; Ha, Hb and Hc. Among these, Ha, a stationary proton near to the electronegative nitrogen atom, appears in the mid field region of 5.52 ppm. It is clear from the structure that the geminal protons Hb and Hc are not in the same space of the pyrazoline ring, so Hb is shifted by the next benzene ring slightly to the left at a chemical shift of 4.03 ppm and Hc is located at a chemical shift of 3.20 ppm. The –CH_2- hydrogens show a quartet signal at 4.21 ppm and the methyl group appears as a triplet at 1.49 ppm.

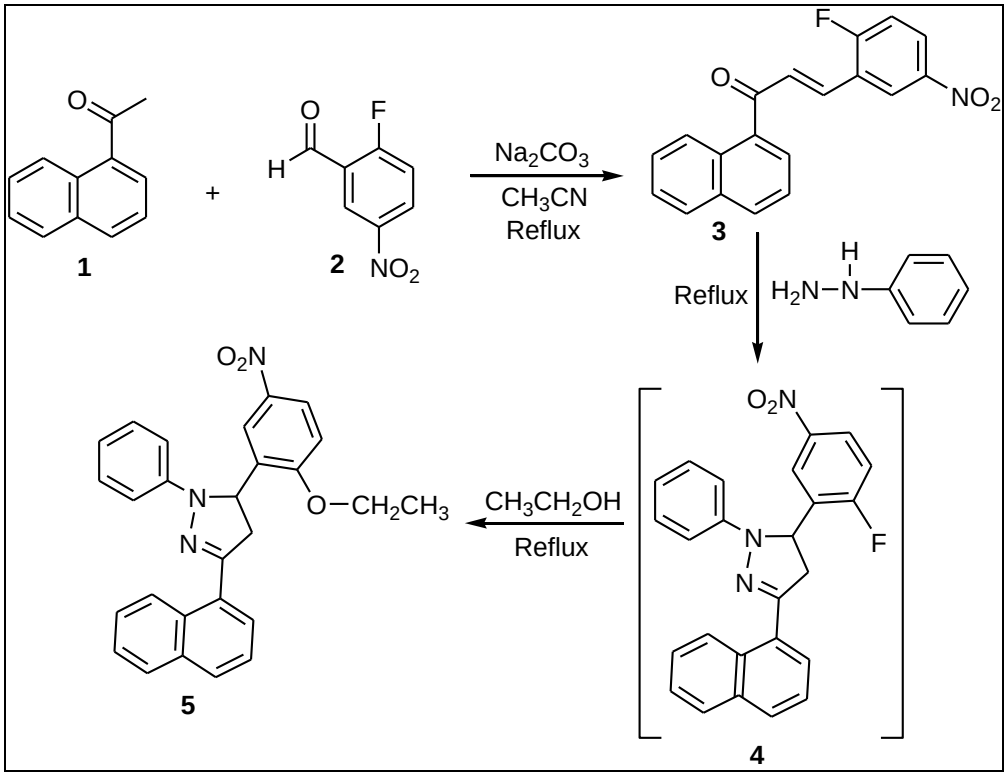

Scheme 1. Synthetic protocol of NPENP 5.

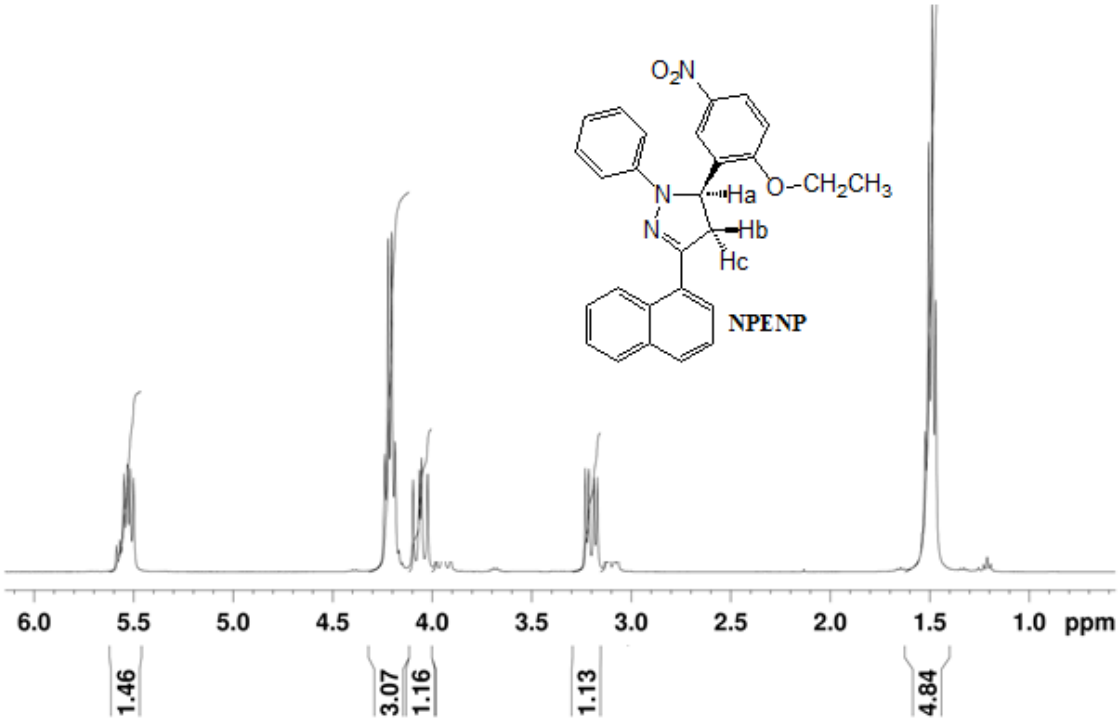

Figure 3. The aliphatic ^{1}H NMR spectrum ($CDCl_3$) of NPENP.

3.2 Optical Spectroscopy

The NPENP is a chromophoric π-system composed of three aryl substituents in the 1-, 3- and 5- positions of pyrazoline ring atoms. As shown in Figure 4, this compound exhibits two prominent bands in all selected solvents, appearing at 298-312 nm and 373-391 nm, respectively, and the molar absorption coefficient values are in the same range of 6×10^4 $M^{-1}cm^{-1}$. The shorter wavelength is ascribed to a localized aromatic π-π^* transition and the long wavelength is attributed to ICT transitions [24]. However, in water there is a distinct bathochromic shift in the

absorption maxima compared to those in non-aqueous solvents. The shift in magnitude of the peak position according to the polarity of the medium suggests that the ground state of the molecule is polar.

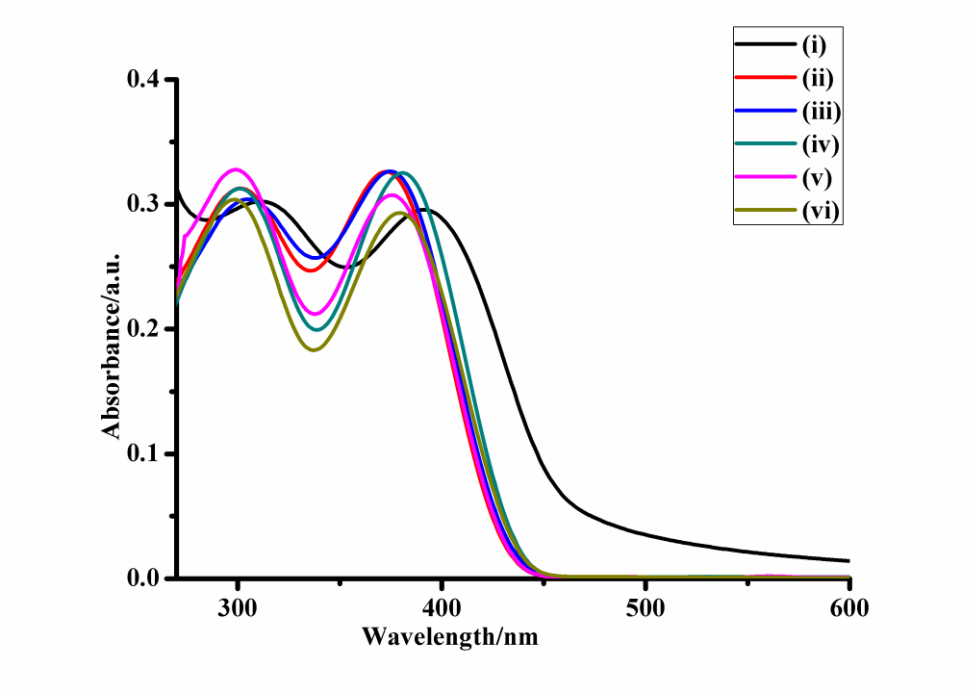

Figure 4. The absorption spectra of NPENP in (i) Water (ii) Methanol (iii) Acetonitrile (iv) Dioxane (v) Ethyl acetate and (vi) Tetrahydrofuran.

Even though the molecule is designed in such a way that the aryl rings in this compound can communicate electronically through the pyrazoline π-system to produce an analytically useful signals, the question why the title compound is not fluorescent is crucial. In particular, the UV absorption spectra of NPENP in solvents of differing polarity clearly indicate that there is an intramolecular charge transfer throughout the system in ground state.

3.3 X-ray crystallography

To study the packing properties of NPENP, good-quality single crystals suitable for X-ray analysis were grown in ethanol solvent by slow evaporation at ambient conditions and were found to have a monoclinic crystal lattice with the $P2_{1/C}$ space group. The molecular view of FNPFE is shown in Figure 5. A summary of crystallographic data collection parameters and refinement parameters are compiled in Table 1.

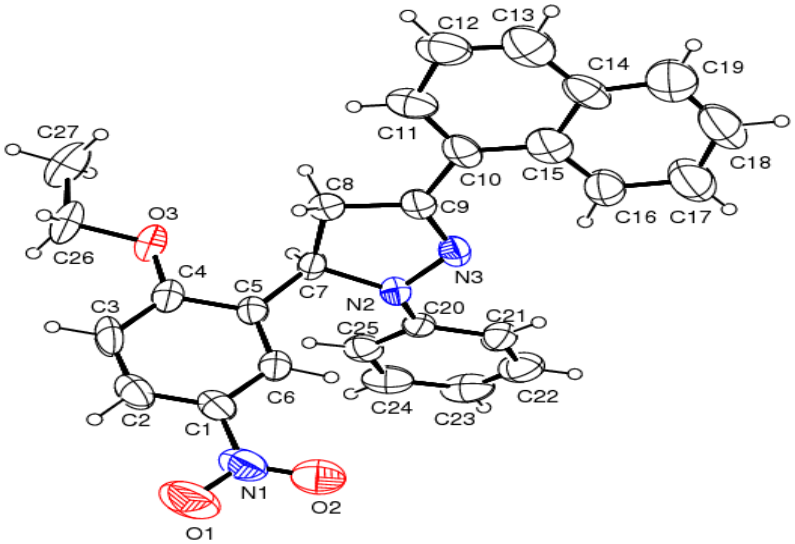

Figure 5. ORTEP diagram and atom labelling of NPENP.

Table 1. Crystal data and parameters of X-ray diffraction experiment for NPENP.

Empirical formula	$C_{27}H_{23}N_3O_3$
Formula weight	437.48
Temperature	293(2) K
Wavelength	0.71073 Å
Crystal system	Monoclinic
Space group	P21/c
Unit cell dimensions	a = 15.8696(14) Å α= 90 b = 9.9425(9) Å β= 111.652(4)° c = 15.5068(14) Å γ = 90°
Volume	2274.1(4) Å3
Z	4
Density (calculated)	1.278 Mg/m^3
Absorption coefficient	0.085 mm^{-1}
F (000)	920
Crystal size	0.350 × 0.300 × 0.250 mm^3
Theta range for data collection	2.470 to 24.095°
Index ranges	-14<=h<=18, -11<=k<=11, -17<=l<=17
Reflections collected	21823
Independent reflections	3547 [R(int) = 0.0896]
Completeness to theta = 24.095°	98.1 %
Absorption correction	Semi-empirical from equivalents
Maximum and minimum transmission	0.9799 and 0.9702
Refinement method	Full-matrix least-squares on F2
Data / restraints / parameters	3547 / 76 / 298
Goodness-of-fit on F2	1.020
Final R indices [I>2 sigma(I)]	R1 = 0.0975, wR2 = 0.2547
R indices (all data)	R1 = 0.2052, wR2 = 0.3282
Extinction coefficient	n/a
Largest diff. peak and hole	0.629 and -0.244 e Å-3

One phenyl moiety, a naphthalene ring and a substituted phenyl ring are bonded to the pyrazoline ring at the atoms of N2, C9 and C7, respectively. The N2—N3 (1.398 Å) (6) and C9—N3 (1.283 Å) (7) bonds have pure single- and double-bond character, respectively. The torsion angle at (C9-C10-C15-C14) is -177.4 (5)º, which shows that the molecular structure adopts a *trans* configuration about the C9=N3 bond. The dihedral angle between the pyrazoline and substituted phenyl ring (C4-C5-C7-C8) is found to be 74.5 (6)º. The conformation of the naphthalene (C8-C9-C10-C11) and phenyl unit (C21-C20-N2-N3) with respect to the pyrazoline ring can be indicated by the torsion angles -1.3 (8)º and 23.1 (7)º, respectively. Even though the N2 atom is not involved in conjugation with the pyrazoline double bond, it is sp^2 hybridized with its lone-pair electrons delocalized through conjugation with the adjacent phenyl group, as shown by the N2–C20 bond length (1.387 Å) (7). This bond length is shorter than a C–N single bond (1.47 Å) and slightly longer than a C=N bond (1.30 Å). The sum of the three angles around N2 atom is 350º, which clearly indicates the pyramidal disposition of the bonds at the atom N2. The C–C bond distances in its aromatic rings are in the normal range of 1.32-1.45 Å, which is characteristic of delocalized aromatic rings [19]. The selected bond length, bond angles and torsion angles are presented in Table 2.

Table 2. Selected geometrical parameters by X-ray and theoretical calculations at B3LYP/6-31G level of theory in ground state and excited state for NPENP.

		Distance Å	
Bond	X-ray	Ground state	Excited state
C9–N3	1.28 (7)	1.33	1.31
N2–N3	1.39 (6)	1.35	1.40
C20–N2	1.38 (7)	1.38	1.44
C5–C7	1.49 (7)	1.51	1.50
C9–C10	1.49 (9)	1.44	1.46
C4–O3	1.33 (7)	1.42	1.49
Bond		Angle (º)	
C8-C9-C10	121.8 (6)	-106.3	-103.3

C9-N3-N2	109.6 (6)	110.1	111.2
C20-N3-N2	116.8 (5)	119.9	117.9
C5-C7-C8	113.0 (4)	114.7	112.3
O3-C4-C5	114.4 (5)	116.2	115.9
C11-C10-C9	117.0 (6)	125.4	118.6
N3-C9-C10	125.2 (6)	123.7	124.5
Torsion angle		Angle (º)	
C9-C10-C15-C14	-177.4	178.5	178.6
C4-C5-C7-C8	74.4	127.6	129.0
C8-C9-C10-C11	-1.3	5.7	-11.6
C21-C20-N2-N3	23.0	-167.4	10.6
N3-C9-C10-C15	1.9	5.8	-11.5

Table 2. Contd.

The 5-substituted phenyl ring on the asymmetric carbon of a pyrazoline moiety (C7) is oriented in such a manner that one of its hydrogen atoms (H27A) is located almost on top of the pyrazoline moiety at 2.6131 Å distance from the center of the pyrazoline ring. The angles around the asymmetric carbon are 111.7º (4) (N2–C7–C5), 101.9º (4) (N2–C7–C8), 113.0º (4) (C5–C7–C8), 110.0º (N2–C7–H7), 110.0º (C5–C7–H7), 110.0º (C8–C7–H7). The bond length of the C–C single bond bridging the naphthalene, the 5-substituted phenyl group and the pyrazoline ring (C9–C10, C5–C7) is calculated to be 1.49Å (9, 7). This bond is significantly shorter than a typical C–C single bond of 1.54Å. This reflects an efficient charge delocalization over the pyrazoline π-system allowing electronic interaction between the attaching groups as they are electronically separated. Analogously it is clear that the presence of an electron attracting nitro group and electron donating ethoxy substituent distorts the interatomic distances so that the bond length of C4–O3 reduces to 1.339 (7) Å , in contrast to the normal C–O bond of 1.43 Å.

The mean plane of the pyrazoline ring (N2/N3/C7/C9) makes dihedral angles of 16.3 (7), 1.3 (8) and 10.6 (7)^0 with the phenyl ring (C20–C25), naphthalene ring (C10–C11), and substituted phenyl ring, respectively, and it exists in a flattened envelope conformation with one carbon atom (C8) deviating from the mean plane of the remaining four atoms. Regarding the crystal packing, there are significant intramolecular C2–H2....O1 (2.34 Å), C6–H6....N2 (2.455 Å), C6–H6....O2 (2.408 Å), C7–H7....O3 (2.478 Å), C21–H21....N3 (2.426 Å) hydrogen bonds-forming pseudo five membered ring [20]. The molecular conformation is further stabilized by ten intramolecular hydrogen bonds which involve all the fragments in NPENP, serving as both acceptors and donors in a set of head to tail fashion. The C8–H8....O3 (3.005 Å, x, y, z), C16–H16....N3 (2.133 Å, x, y, z), C25–H25....O2 (2.741 Å, -x+1, +y+1/2, -z+1/2+1), C27–H27....O2 (2.527 Å, x, +y+1, +z), C19–H19....O1 (2.616 Å, x-1, -y+1/2+1, +z-1/2) hydrogen bonding networks play an important role in bringing the molecules in close proximity to each other [21]. Among these it is clear that three hydrogen bonds (O2...H27, O2...H25 and O2...H6) are trifurcated since they share the same oxygen (O2) atom.

The bond lengths between these atoms are 2.6131 Å, 2.869 Å and 2.424 Å respectively. Similarly another four hydrogen bonds (O3...H8, O3...H7 and N3...H16, N3...H21) are bifurcated and their bond lengths are 2.996, 2.477, 2.223, and 2.446 Å, respectively, (Table 3).

Table 3. Parameters for the intra- and inter molecular hydrogen bonding.

D–H	D…..A	H….A	D–H….A
C2–H2 (0.93)	C2….O1 (2.66)	H2….O1 (2.36)	C2–H2….O1 (2.34)
C6–H6 (0.93)	C6…..N2 (2.83)	H6….N2 (2.48)	C6–H6….N2 (2.45)
C7–H7 (0.98)	C7….O3 (2.67)	H7….O3 (2.47)	C7–H7….O3 (2.47)
C8–H8A (0.97)	C8….O3 (3.08)	H8A….O3 (2.99)	C8–H8A….O3 (3.00)
C21–H21 (0.93)	C21….N3 (2.75)	H21….N3 (2.44)	C21–H21….N3 (2.42)
C16–H16 (0.93)	C16….N3 (2.89)	H16….N3 (2.22)	C16–H16….N3 (2.13)
C25–H25 (0.93)	C25….O2 (3.70)	H25….O2 (2.86)	C25–H25….O2 (2.74)
C27–H27 (0.96)	C27…..O2 (3.37)	H27A….O2 (2.61)	C27–H27A….O2 (2.52)
C19–H19 (0.93)	C19….O1 (3.49)	H19….O1 (2.72)	C19–H19….O1 (2.61)
Donor–Hydrogen	*Donor…Acceptor*	*Hydrogen….Acceptor*	*Donor–Hydrogen…Acceptor*

The establishment of CH–π interactions consequently result in the stacking of the NPENP molecules to be packed as a crystal along *b* axis like a chair as shown in Figure 6. The molecular packing diagram shows two layers of molecules, which are independently arranged in the unit cell. In the extended structure of NPENP it is clear that intermolecular CH–π interactions within each unit and π....π contact between the individual chain of a single molecule in a zig-zag manner to produce chains running parallel to each other.

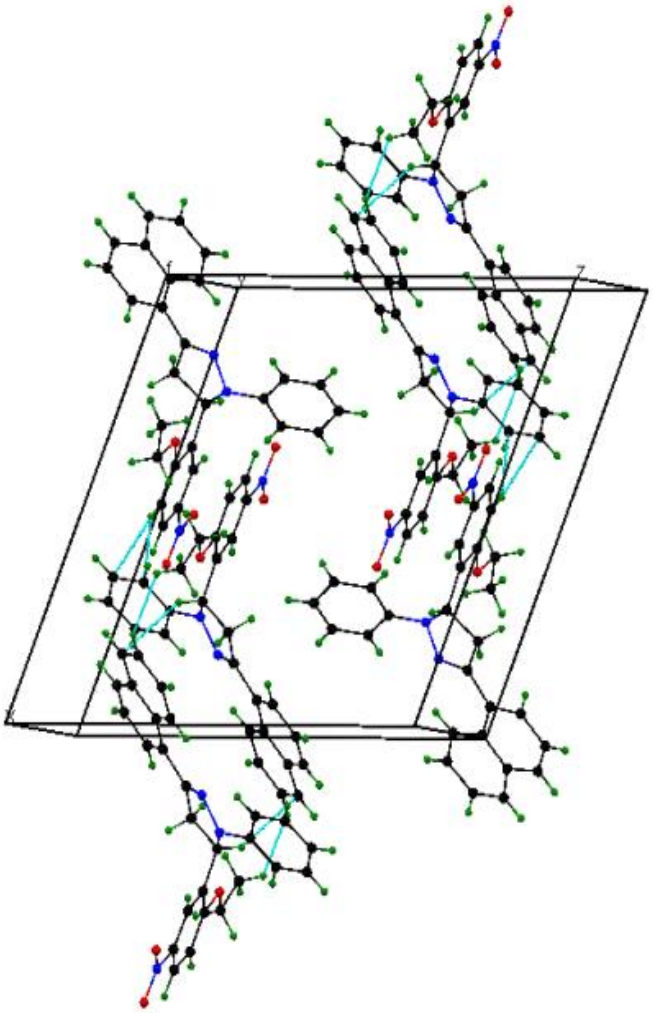

Figure 6. Packing diagram of NPENP viewed along *b* axis.

3.4 Computational details

The DFT functional B3LYP coupled with the 6-31G basis set was used to perform geometry optimizations in *vacuo*, for comparing the XRD data with theoretical parameters. There are some differences between the experimental values and the calculated data as the geometry of the solid-state structure is subject to intermolecular forces, such as van der Waals interactions, crystal packing forces and hydrogen-bond forces [22], but the calculated data corresponds to the isolated molecule in gas phase.

As discussed previously for the crystal structure, the N2—N3 bond length (1.351 Å) is slightly lower than the experimental value; surprisingly C9—N3 (1.335 Å) shows deviation from the typical C=N behavior of the pyrazoline ring (~1.28 Å) in solid state. The bond length of sp^2 hybridized N2 atom and the phenyl attaching carbon C20 is in good agreement with the experimental value, but the sum of the three angles around N2 atom is exactly 360º indicating that the bonds meeting at N2 are almost coplanar in gaseous phase and this high degree of coplanarity invokes electronic transitions in ground state (see Figure 7).

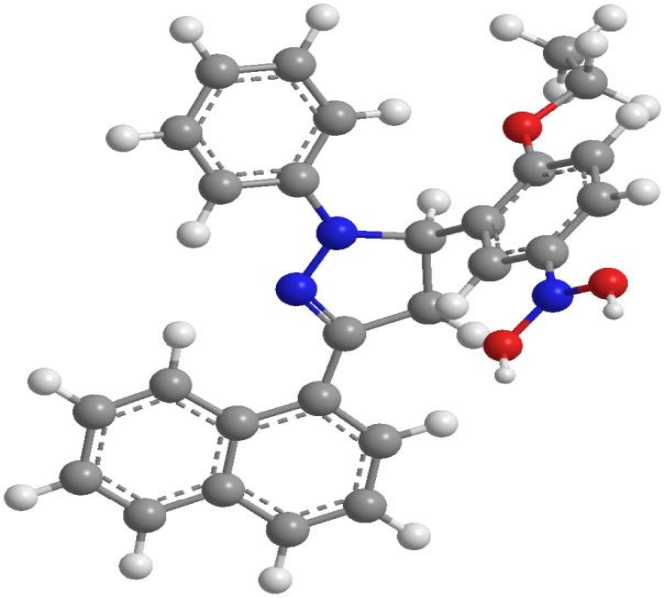

Figure 7. The optimized molecular geometry of NPENP in its ground state at B3LYP/6-31G level.

The calculated torsion angle at C9-C10-C15-C14 is found to be 178.597° and the difference of about ±180° from the experimental value corresponds to a rotation of 180° about the C9-C10 axis of the naphthalene ring, which does not affect the molecular stability. The bond length of the C9–C10 single bond bridging the naphthalene ring (1.44 Å) is found to be lower than that of the experimental value (1.49 Å) and also lower than the C5–C7 bond bridging the substituted phenyl group (1.51 Å). It was noticed that the distance between the pyrazolinic nitrogen connecting to the attaching carbon of the phenyl ring is shorter (1.388 Å) than a normal C–N single bond (1.47 Å). It implies that there is a chance for high degree electron density delocalization from the π-bridge towards the naphthalene and phenyl rings, which is crucial for the highly enhanced ICT character in ground state. The computational analysis of the frontier molecular orbitals (see **Figure 8**) provides more insightful information on the energies of occupied and virtual front orbitals and their influence on the excitation and emission properties of NPENP.

Figure 8. Frontier orbitals of NPENP calculated by the TD-DFT/ B3LYP/6-31G method on ground and excited state (i) $NPENP_{HOMO}$ (G.S) (ii) $NPENP_{HOMO-1}$ (G.S) (iii) $NPENPE_{LUMO}$ (G.S) (iv) $NPENP_{LUMO+1}$ (G.S) (v) $NPENPE_{HOMO}$ (EX) (vi) $NPENP_{HOMO-1}$ (EX) (vii) $NPENP_{LUMO}$ (EX) (viii) $NPENP_{LUMO+1}$ (EX).

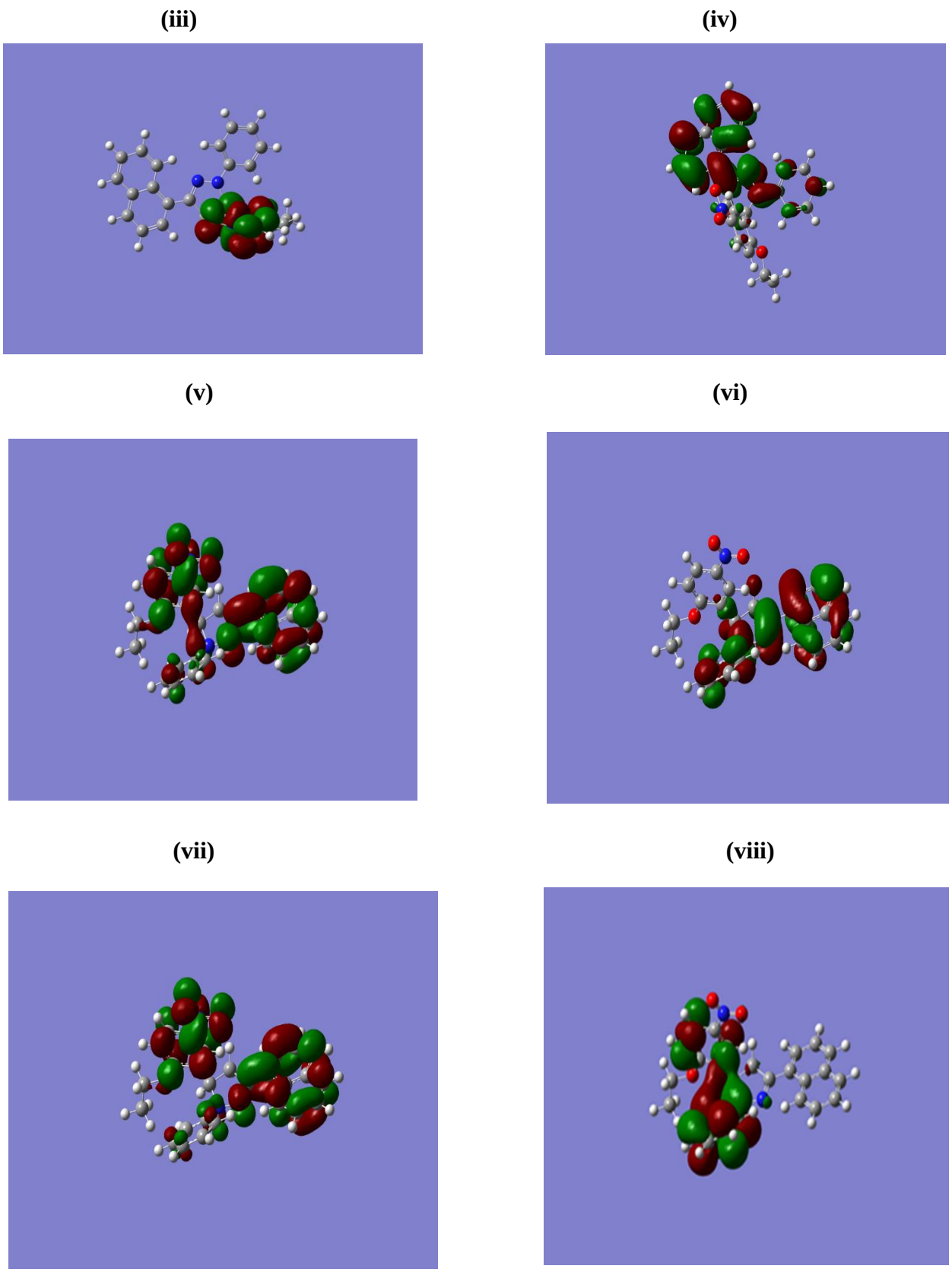

Figure 8. Contd.

The energies of HOMO, LUMO and their neighboring orbitals are all negative, which indicates the stability of NPENP in ground state, whereas the molecule is instable in excited state. In ground state the HOMOs are mainly localized on the naphthalene, pyrazoline and 1-phenyl rings and the LUMO is fully populated on the 5-substituted phenyl ring. By contrast, the contribution of naphthalene and pyrazoline is increased in LUMO+1 and the small energy gap (0.053 eV) underlines the highly delocalized nature of NPENP in ground state. From the figure it is observable that

the bent $–CH_2-CH_3$ group has no charge density distribution, neither on the HOMO nor on the LUMO levels of NPENP in both ground and excited state.

On the other hand, there is a large distortion in the geometry of NPENP in excited state accompanied by unfavorable changes in the basic dimensions, particularly in the bond length and bond angles involving the pyrazoline ring. There is perceptible lengthening of N2—N3 (1.407 Å), N2—C20 (1.447 Å) and C9-C10 (1.463 Å) bond length in excited state geometry. The sum of the bond angles at N2 is found to be 347.28º and is considerably distant from the planarity. The dihedral angle C11-C10-C9-C8 (179.12º) is an indication of coplanar orientation of the pyrazoline and naphthalene rings in excited state while both the phenyl and substituted phenyl rings are folded slightly from their attached pyrazoline ring with torsion angles of 10.617º (C21-C20-N2-N3) and -50.496º (C4-C5-C7-C8), respectively (see Figure 9).

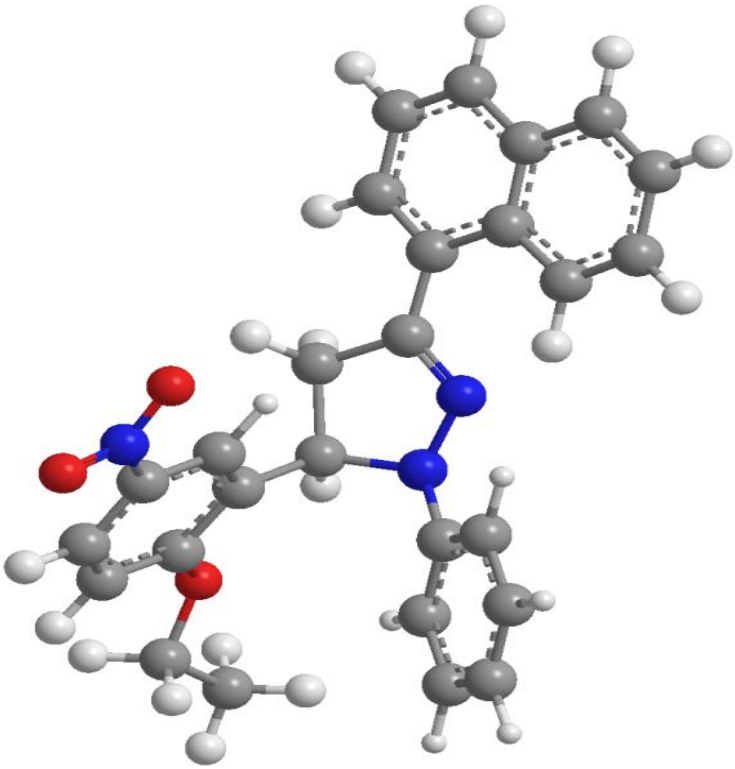

Figure 9. The optimized molecular geometry of NPENP in excited state at B3LYP/6-31G level.

As shown, for NPENP in excited state the electron densities of HOMO are mainly located on the naphthalene ring; there is an electron distribution from the substituted phenyl ring to the pyrazoline ring, except in case of the C8 carbon and a small node on the 1-phenyl ring. The increase in electron density on the left part including the pyrazoline and 1-phenyl rings was observed for HOMO-1 in excited state, and the LUMO is equally delocalized on the naphthalene and 5-substituted phenyl rings with a small contribution on C-N=N. The LUMO +1 looks like a flow of electrons from the 1-phenyl ring, including N2-C7, and as a separated cloud on the center of the 5-substituted phenyl ring. Compared to the MOs of the ground state (S_0) the contribution of the 5-substituted phenyl ring is greater in excited (S_1) state. This can increase the electron density on the conjugated back bone and its steric effects cause distortion of the conjugated back bone [23]. On the other hand, it is clear that the phenyl group at N2 also destroys the coplanar character of the conjugated backbone in excited state. This ensures that a steric effect arises due to the distorted geometry of NPENP hampering the delocalization of a/ the lone pair of electrons of –N3 atom, and this may also disturb the conformational stability of C=N–N which in turn will cause a decrease in conjugation, and thereby decrease in charge transfer throughout the system and make the LUMO-HOMO energy gap wider (0.134 eV).

4. Conclusion

Combining computational studies with single crystal X-ray diffraction facilitates a deeper understanding of the geometry of NPENP in solid and gaseous state. The analysis of the molecular geometry of NPENP in ground state exhibits a very good agreement with the experimental data. Considering the geometry of NPENP in excited state, one can clearly find that non-planarity and proximity of atoms play an important role in hindering the delocalization of π electrons throughout the system. The high molar absorptivity of NPENP underlines the importance of its mother dye NPFNP in the determination of alcohols and phenolic derivatives.

5. Acknowledgements

Beena Varghese would like to thank SQU for a PhD scholarship. We also acknowledge SAIF (IIT, Madras, India) for providing crystallographic data.

Supporting Information

Crystallographic data for the structure reported in this article have been deposited with the Cambridge Crystallographic Data Center with the deposition number 1056209. A copy of the data can be obtained free of charge from the Director, CCDC, 12 Union Road, Cambridge CB2 IEZ, UK; fax: +44(0)1222-336033; email: deposit@ccdc.cam.ac.uk.

References

1. Dai, Y., Guo, M., Peng, J., Shen, W., Li, M., He, R., Zhu, C. and Lin, S.H. Noncovalent interaction and its influence on excited-state behaviour: A theoretical study on the mixed coaggregates of dicyanonaphthalene and pyrazoline. *Chemical Physics Letters*, 2013, **556**, 230-236.
2. Anam, F., Abbas, A., Lo, K.M., Rehman, Z.U., Hameed, S. and Naseer, M.M. Homologous 1,3,5-triarylpyrazolines: synthesis, CH….π interactions guided self-assembly and effect of alkyloxy chain length on DNA binding properties. *New Journal of Chemistry*, 2014, **38**, 5617-5625.
3. Lone, I.H., Khan, K.Z. and Fozdar, B.I. Synthesis, Physicochemical properties, antimicrobial and antioxidant studies of pyrazoline derivatives bearing a pyridyl moiety. *Medicinal Chemistry Research*, 2014, **23**, 363-369.
4. Havrylyuk, D., Zimenkovsky, B., Karpenko, O., Grellier, P. and Lesyk, R. Synthesis of pyrazoline- thiazolidinone hybrids with trypanocidal activity. *European Journal of Medicinal Chemistry*, 2014, **85**, 245-254.
5. Wang, H.Y., Shi, J.J., Chen, G., Xu, X.P. and Ji, S.J. Synthesis and characteristics of novel benzothiazoyl-pyrazoline derivatives containing carbazole. *Synthetic Metals*, 2012, **162**, 241-246.
6. Kumar, C.K., Trivedi, R., Kumar, K.R., Giribabu, L. and Sridhar, B. Synthesis, Characterization, electrochemistry and optical properties of new 1,3,5-trisubstituted ferrocenyl pyrazolines and pyrazoles containing sulfonamide moiety. *Journal of Organometallic Chemistry*, 2012, **718**, 64-73.
7. Shi, H-P., Dai, J.X., Zhang, X.F., Xu, L., Wang, L., Shi, L.W. and Fang, L. Experimental and theoretical study of two new pyrazoline derivatives based on dibenzofuran. *Spectrochimica Acta Part A: Molecular and Biomolecular Spectroscopy*, 2011, **83**, 242-249.
8. Singh, P., Negi, J.S., Singh, K., Pant, G.J., Rawat, M.S.M. and Joshi, G.C. Synthesis and structure dependent photophysical properties of novel 2-pyrazolines. *Synthetic Metals*, 2012, **162**, 1977-1980.
9. Wang, S.Q., Gao, Y., Wang, H.Y., Zheng, X.X., Shen, S.L., Zhang, Y.R. and Zhao B.X. Synthesis, X-ray crystal structure and optical properties of novel 1,3,5-triarylpyrazoline derivatives and the fluorescent sensor for Cu^{2+}. *Spectrochimica Acta Part A: Molecular and Biomolecular Spectroscopy*., 2013, **106**, 110-117.
10. Zhao, P., Zhou, S., Guo, Z. and Zhu Y. Crystal structure, Spectral properties and comparative studies on a 2-pyrazoline derivative. Spectrochimica Acta Part A: Molecular and Biomolecular Spectroscopy, 2012, **94**, 65-71.
11. Zeng, Y.M., Chen, S.Q. and Liu, F.M. Synthesis and crystal structure of new thiazolyl-pyrazoline derivatives bearing 1, 2, 4-triazole moiety. *The Journal of Chemical Crystallography*, 2012, **42**, 24-28.
12. Chinnaraja, D., Rajalakshmi, R., Srinivasan, T., Velmurugan, D. and Jayabharathi, J. Spectral studies of 2-pyrazoline derivatives: Structural elucidation through single crystal XRD and DFT calculations. *Spectrochimica Acta Part A: Molecular and Biomolecular Spectroscopy*, 2014, **124**, 30-33.
13. Assaf, P., Katzhendler, J. and Haj-Yehia, Al. 2- (4-carboxyphenyl) -6 -N, N-diethyl amino benzofuran; a useful reagent for the sensitive determination of alcohols by high performance liquid chromatography with fluorimetric detection. *The Journal of Chromatography A*, 2000, **869**, 243-250.
14. Varghese, B., Al-Busafi, S.N., Suliman, F.O. and Al-Kindy, S.M.Z. Study on the spectral and inclusion properties of a sensitive dye, 3-naphthyl-1-phenyl-5-(5-fluoro-2-nitrophenyl)-2-pyrazoline, in solvents and β-cyclodextrin. *Spectrochimica Acta Part A: Molecular and Biomolecular Spectroscopy*, 2015, **136**, 661–671.
15. Sheldrick, G.M. SHELXTL, v5 Reference Manual; Siemens Analytical X-Ray Systems: Madison, WI, 1997.
16. Wilson, A.J. *International Table for X-ray Crystallography*; Kluwer Academic, Dordrecht: The Netherlands, 1992, Vol.C: Tables 6.1.1.4 (pp. 500-502) and 4.2.6.8 (pp.219-222).
17. Becke, A.D. Density-functional exchange-energy approximation with correct asymptotic behaviour. *Physical Review A*, 1988, **38**, 3098- 3100.

18. Lee, C., Yang, W. and Parr, R.G. Development of the Colle-Salvetti correlation-energy formula into a functional of the electron density. *Physical Review B*, 1988, **37**, 785-789.
19. Oliva, J.M., Allan, N.L., Schleyer, P.V.R., Vinas, C. and Teixido, F. Strikingly Long C….C distances in 1, 2-Disubstituted *ortho*- carbenes and their Dianions. *Journal of the American Chemical Society*, 2005, **127**, 13538-13547.
20. Gong, Z-L., Zheng, L-W., Zhao, B-X., Yang, D-Z., Lv, H-S., Liu, W-Y. and Lian S. The Synthesis, X-ray crystal structure and optical properties of novel 1, 3, 5- triaryl pyrazoline derivatives. *Photochemistry and Photobiology*, 2010, **209**, 49-55.
21. Chamas, Z., Marchi, E., Presson, B., Aubert, A., Ceroni, P. and Mamane, V. Synthesis and solid state fluorescence properties of pentacyclic 7-substituted-indeno [1', 2': 4, 5] pyrido [2, 1-a] isoindol-5-ones. *RSC Advances*, 2015, **5**, 2715-2723.
22. Thompson, H.P.G. and Day, G.M. Which conformations make stable crystal structures? Mapping crystalline molecular geometries to the conformational energy landscape. *Chemical Sciences*, 2014, **15**, 3173-3182.
23. Demachy, I. and Volatron F. Hyperconjugation versus steric effects: *Ab* Initio study of the B_2D_4 systems (D= H, CH_3, NH_2, OH, F, Cl). *Journal of Physical Chemistry*, 1994, **98**, 10728-10734.
24. Varghese, B., Al-Busafi, S.N., Suliman, F.O and Al-Kindy, S.M.Z. Synthesis, spectroscopic characterization and photophysics of a novel environmentally sensitive dye 3-naphthyl-1-phenyl-5(4-carboxyphenyl)-2-pyrazoline. *Journal of Luminescence*, 2015, **159**, 9-16.

Received 7 September 2016
Accepted 6 November 2016